Research Article

Received: 18 June 2021 Revised: 25 August 2021 Accepted article published: 1 September 2021 Published online in Wiley Online Library:

(wileyonlinelibrary.com) DOI 10.1002/jctb.6904

Removal of hexavalent chromium (Cr(VI)) from aqueous solution using acid-modified poultry litter-derived hydrochar: adsorption, regeneration and reuse

Bashir Ghanim,[a,b] James J Leahy,[a,b] Thomas F O'Dwyer,[a,b] Witold Kwapinski,[a,b] J Tony Pembroke[a,b] and John G Murnane[c*]

Abstract

BACKGROUND: Chromium (Cr) is widely used in industrial processes and is considered a major source of pollution when released to the environment. Of particular concern, hexavalent chromium (Cr(VI)) is amongst the most toxic heavy metals affecting human health and living organisms when fugitive emissions contaminate aqueous environments. Consequently, its removal and recovery are priorities for environmental remediation in the context of the circular economy. In this study, modified hydrochar (MHC) was generated by hydrothermal carbonisation of acid-treated (H_2SO_4) poultry litter (PL) and investigated for its ability to adsorb Cr(VI) from aqueous solution in batch studies. Recovery of Cr(VI) and the regeneration potential of MHC were also evaluated.

RESULTS: Results indicated that Cr(VI) adsorption was strongly pH dependent, demonstrating an inverse relationship between solution pH and Cr(VI) uptake. A maximum adsorption capacity of 26.2 mg g^{-1} was achieved in 90 min at pH 2. Under optimal conditions, adsorption kinetics followed a pseudo-second-order kinetic model and the adsorption isotherm fitted most closely with the Langmuir model. Thermodynamic studies indicated that the adsorption process of Cr(VI) onto the MHC was exothermic and spontaneous. Regeneration studies demonstrated that the MHC can be re-used up to four times without significant loss of capacity to adsorb Cr(VI).

CONCLUSIONS: Modified PL hydrochar offers potential as a low-cost, environmentally friendly solution for Cr(VI) adsorption in wastewater treatment applications. The ability of Cr(VI) to desorb from MHC demonstrates strong potential for Cr(VI) recovery and regeneration of the adsorbent.

Keywords: poultry litter; hydrochar; adsorption; desorption

INTRODUCTION

Industrial processes account for a significant level of both organic and inorganic pollutant emission to air, soil and water.[1,2] In particular, contamination of natural water resources with heavy metals has become increasingly problematic due to adverse impacts on the environment, causing serious problems worldwide with a cumulative and harmful effect on human health.[3] While some heavy metals from natural sources enter the environment, industrial release accounts for the largest proportion.[2] Heavy metals such as Cr, Cd, Hg, As and Pb are harmful to human health[4] and their toxicity to living organisms depends greatly on their biodegradability and bioavailability.[5] Chromium (Cr) is a natural element found in soil, animals and plants and in its most stable form, Cr(III) can be an essential element in human nutrition.[6,7] Cr is also widely used in industrial processes such as leather tanning, metal polishing, paint manufacturing, electroplating and other industries, and is considered a major source of environment pollution in waste streams.[3,8] Cr(VI) in particular is amongst the most toxic heavy metals for humans and can be found in high concentrations in the receiving environment due to its mobility.[5,9] More recently, with a shift in emphasis from a linear to a circular economy, the recovery and valorisation of secondary metal resources have gained increased significance for the development of low-

* *Correspondence to: JG Murnane, School of Engineering, University of Limerick, Limerick, Ireland. E-mail: john.murnane@ul.ie*

a *Department of Chemical Sciences, School of Natural Sciences, University of Limerick, Limerick, Ireland*

b *Bernal Institute, University of Limerick, Limerick, Ireland*

c *School of Engineering, University of Limerick, Limerick, Ireland*

carbon technologies. In the EU for example annual demand for Cr in the wind energy sector, identified as a priority in the EU Strategic Energy Technology plan, is projected to be 10 000 t by 2030.[10] This has prompted new research such as Cr recovery from stainless steel slags while carbonating the remaining matrix material for the production of building materials[11] and the development of new circular business models for low-grade secondary raw materials, including Cr-rich sludges.[12]

A range of water treatment and soil remediation processes for the removal of toxic heavy metals from industrial discharges have been studied.[5,13] Of these, adsorption offers several advantages such as operational simplicity, high removal efficiency, economic viability and potential re-use and recycling of waste materials.[4,8] In this regard, biomass/biowaste and their derivative residues have been studied as adsorbents for contaminants and have been shown to be effective for removal of metals from soils and wastewaters.[2,5] Waste-derived materials such as low-cost agricultural biomass, sewage sludge and industrial effluents can be converted by thermal treatment to biochar or hydrochar to act as effective adsorbents for a range of metals from wastewater.[14,15] While these biosorbents have different physicochemical characteristics, their ability to adsorb contaminants from a variety of waste streams, including heavy metal removal, is mainly attributable to their surface characteristics, oxygenated functional groups, high cation-exchange capacity, aromatic carbon structure and high mineral content.[16] They have many advantages over conventional treatment systems (e.g. chemical precipitation, coagulation–flocculation, flotation and cementation) in that the feedstocks are naturally occurring, of low cost and readily available in large quantities; however, challenges in their regeneration and reuse as well as their ability to treat complex waste streams still remain.[16]

To improve biomass/biowaste adsorption capacity, many methods, including chemical modification and thermochemical treatment, have been used to produce adsorbents with high removal efficiencies. Among the thermochemical methods used for stabilising biowaste, hydrothermal carbonisation (HTC) involves mixing biomass/biowaste with water and heating the slurry to treatment temperatures between 180 and 260 °C for residence times ranging from a few minutes to several hours under self-generated pressure.[17] HTC has gained considerable interest as an effective thermal treatment for the conversion of cheaper material into valuable products such as hydrochar (HC).[18] HC has several potential applications and can be directly used as a fuel, for example by converting poultry litter into a solid fuel similar to coal,[19] as a soil amendment by increasing its long-term carbon and nutrient content and water retention capacity,[20] or as an adsorbent for environmental remediation such as heavy metal, phosphate, organic pollutant and pathogen removal from contaminated wastes.[21] The chemical and physical properties of HC as well as its adsorption characteristics differ significantly from that of the starting material.[21] The use of HC as an adsorbent for the remediation of soil and water contaminated with organic and inorganic contaminants has attracted much interest in recent years due to its low cost, abundant availability and relative ease of preparation.[22] The efficient removal of contaminants depends on the properties of HC and pollutants. The adsorption capacity of the adsorbent largely depends on its morphology and surface chemistry which are affected by the treatment conditions.[21,23] Therefore, selection of the optimum HCs produced at different treatment conditions is critical. Although HC is characterised by small pore size and limited surface area,[24] it has various surface functional groups such as hydroxyl, carboxyl, amino and others which can play a role in contaminant removal.[21] Thus, enhancement of the adsorption properties of HC can be achieved through modifying its surface functionality, including chemical modification, activation and impregnation.[7,25] Chemical modification is a very useful method which can provide the desired adsorption characteristics by forming and/or exposing more active sites.[2] Acid modification is applied using various oxidants, leading to more acidic functional groups on the adsorbent surface and the removal of mineral elements. Treatment of biochar using H_2SO_4 has been reported in the literature, improving its catalytic activity[26] and increasing its capacity for contaminant removal, such as removal of the antibiotic sulfamethazine frequently found in soil and water environments[27] and removal of Al from acidic soils.[28] Typically, acid modification is conducted by treating the HC in acid solution[21] or as in the case of the study reported here, by treating HC with H_2SO_4 during the HTC process.

Poultry litter (PL) is a widely available agri-biowaste material which consists of faeces, dropped feed and feathers and may contain bedding material and other farming waste.[29] PL is commonly used as an agricultural fertiliser to improve soil fertility; however, some research has been carried out concerning the production of PL HCs for use as a biofuel and/or fertiliser.[17,29] Others have produced and tested HC from PL as an adsorbent without modification.[23,30] Additionally there are some studies that have shown that H_2SO_4 activation enhances the adsorption properties of biochar produced from various feedstocks,[27] but to the best of our knowledge, there is no literature reporting the application of HC prepared by HTC of PL as an adsorbent for Cr(VI) removal.

In the batch experimental study reported here, we examined the potential of H_2SO_4-modified HC (MHC) prepared from PL to adsorb Cr(VI) from aqueous solution, focusing on initial solution pH, Cr(VI) concentrations, contact time and temperature. The study also examined the regeneration potential of MHC and recovery of the adsorbed Cr(VI) in the context of a circular economy approach. A key aim was to investigate whether treatment of the PL-derived HC with H_2SO_4 had a beneficial effect on its overall capacity to adsorb Cr(VI).

MATERIALS AND METHODS

Materials

Samples of PL with straw as the bed material were collected from a commercial poultry farm located near Limerick, Ireland. The collected samples were transferred to the laboratory, prepared according to BS EN 14780:2011, kept in sealed polyethylene bags and stored in a freezer until required. The stored samples used for the experiments were on an as-received basis (ar). Sulfuric acid (H_2SO_4; 95.0–97.0%), potassium dichromate ($K_2Cr_2O_7$), sodium chloride (NaCl), hydrochloric acid (HCl; 37%) and sodium hydroxide (NaOH) were purchased from Sigma-Aldrich.

Adsorbent preparation

The HC used was produced following a typical HTC process and the details of the experimental procedure can be found elsewhere.[24] Briefly, the experiments were carried out using an 8.0 L Parr stirred pressure reactor fitted with a removable glass liner. An electric heater was used to supply the heat to maintain the temperature of the reactor. The heating and cooling rates were the same for each experiment as the same reactor was used for all experiments. The PL (ar) (202.9 g) with a moisture content of 37.3% was loaded into the glass liner with 1 L of distilled water.

Journal of Chemical Technology and Biotechnology published by John Wiley & Sons Ltd on behalf of Society of Chemical Industry (SCI).

The suspension was thoroughly mixed for 30 min and then the pH was adjusted to pH 2 using concentrated H_2SO_4. The glass liner containing the suspension was placed into the stainless steel reactor, sealed and purged with N_2, and the stirring started. The reactor was then heated to 250 °C using a PID controller; the reactor pressure was not controlled but was monitored during the experiments. When the desired temperature was reached inside the reactor, the 2 h residence time was initiated. After the target residence time was achieved, the heating was turned off and the reactor was rapidly cooled to room temperature by immersion in a cold water bath. The reactor was vented of gases at ambient temperature and MHC was recovered as a solid residue by vacuum filtration, followed by drying at 105 °C overnight. For comparison, HC was also prepared with no acid added through the same experiment steps. Each experiment was carried out in duplicate and the HC samples were crushed to <0.75 mm and homogenised before being used as an adsorbent.

Adsorbate preparation

Test solutions of Cr(VI) adsorbate (1000 mg L^{-1}) were prepared by dissolving exact quantities of analytical-grade $K_2Cr_2O_7$ (Aldrich) in deionised water. The solutions used in the subsequent experiments were obtained from serial dilution of the stock solution and their pH values adjusted using 0.1 mol L^{-1} NaOH or HCl solutions.

Characterisation methods

All measurements were carried out in triplicate and the mean values with standard deviations (SDs) reported. Moisture content of the HC was determined by the mass loss of a sample at 105 °C (IS EN 14774-3:2009) and its pH measured according to ASTM D2976-71. The textural properties were evaluated using N_2 adsorption–desorption isotherms at 77 K with an automatic volumetric system (Quantachrome Instruments). Fourier transform infrared (FTIR) spectra were obtained for HC, MHC and Cr(VI)-loaded MHC using a Cary 630 FTIR spectrometer in the wavenumber range from 4000 to 500 cm^{-1}. Surface morphologies were investigated via scanning electron microscopy (SEM) with a Hitachi S-2700. The concentrations of Cr ions were determined using inductively coupled plasma optical emission spectroscopy (ICP-OES) with an Agilent Technologies 5100 ICP-OES and solution pH was measured using a SparkVue 4.1.0 pH meter.

Point of zero charge measurement

The points of zero charge (pH_{pzc}) of MHC and HC were determined using a 50 mL centrifuge tube containing 30 mL of 0.05 mol L^{-1} NaCl. The initial pH in each tube was adjusted to between 2 and 10 by adding either 0.1 mol L^{-1} NaOH or 0.1 mol L^{-1} HCl before the introduction of 0.1 g of adsorbent.[2] The suspensions were then shaken for 24 h in an orbital shaker (IKA 130 Basic) at 293 K, and the final pH of the solutions was determined. The difference between the initial and final pH values was plotted against the initial pH. The pH_{pzc} is the point of intersection of the resulting curve with the abscissa.

Batch adsorption experiments

MHC samples were applied as adsorbents for Cr(VI) removal using batch experiments to determine the most suitable adsorption conditions. The studies were carried out in 50 mL centrifuge tubes on an orbital shaker (IKA 130 Basic) at various pH, contact time, adsorbent dosage, initial adsorbate concentration, ionic strength using NaCl and temperature. After shaking for the selected contact time, the pH was measured and the solutions were filtered through a 0.45 μm syringe filter. The filtrate concentration of Cr ions was determined using ICP-OES. The controls consisted of an adsorbate solution without adsorbent and adsorbent without adsorbate. The adsorption capacity (q_e, mg g^{-1}) of Cr(VI) was obtained using Eqn (1)[2]:

$$q_e = \left(\frac{C_o - C_e}{m}\right) V \quad (1)$$

where C_e and C_o are the equilibrium and the initial Cr(VI) concentrations (mg L^{-1}), respectively, V is the volume of solution (L) and m (g) is the dry mass of the adsorbent.

Solution pH

The effect of pH on the uptake of Cr(VI) onto HC and MHC was explored in the pH range 2–9 using 30 mL of 55 mg L^{-1} Cr(VI) stirred for 24 h with an adsorbent dosage rate of 2 g L^{-1} at 293 K.

Adsorption isotherms

The initial Cr(VI) concentration optimisation was carried out using 30 mL solutions of Cr(VI) with concentrations ranging from 1 to 500 mg L^{-1} at pH of 2 stirred for 24 h with an adsorbent dosage of 2 g L^{-1} at 293 K.

Adsorption kinetics

Adsorption of Cr(VI) onto MHC was conducted as a function of contact time between 5 min and 48 h at pH 2 using 2 g L^{-1} MHC in 30 mL of 55 mg L^{-1} adsorbate solution which was stirred at 293 K.

Adsorption thermodynamics

The impact of temperature on the Cr(VI) adsorption onto MHC was examined at 293, 323 and 348 K using 30 mL of 55 mg L^{-1} Cr(VI) solution at pH 2, stirred for 24 h with an adsorbent application of 2 g L^{-1}.

Ionic strength

The effect of ionic strength was investigated by dispersing 2 g L^{-1} of the adsorbent into 30 mL of 55 mg L^{-1} Cr(VI) at pH 2 and the suspension was stirred for 24 h containing various concentrations of NaCl (0.00, 0.05 and 0.1 mol L^{-1}), at 293 K.

Desorption and regeneration experiments

To determine the reusability of the adsorbents, consecutive adsorption–desorption cycles were studied. Based on adsorption results which indicated that the adsorption of Cr(VI) depended on the solution pH, the use of pH-adjusted distilled water was chosen for desorption of adsorbate from MHC. Distilled water adjusted to pH 12 using 0.1 mol L^{-1} NaOH solution was used to desorb the Cr(VI) ions. The adsorption experiment was conducted using the same protocol described above under optimal conditions; however, the desorption experiment was conducted using a mixture of 2 g of Cr(VI)-loaded MHC and 30 mL of pH-adjusted distilled water (pH 12). After shaking at 293 K for 24 h on an orbital shaker (IKA 130 Basic), the solution was filtered and the adsorbent was washed several times with distilled water until it became neutral, followed by oven-drying at 105 °C and then subjected to the adsorption process again.

Journal of Chemical Technology and Biotechnology published by John Wiley & Sons Ltd on behalf of Society of Chemical Industry (SCI).

RESULTS AND DISCUSSION

Adsorbent characterisation

The structural characteristics (based on FTIR, SEM and Brunauer–Emmett–Teller analyses) of the MHC and HC used in this study, as well their proximate and ultimate analyses, have previously been reported[24] and relevant results are summarised in Table 1. Surface morphology and chemistry are known to significantly influence the effectiveness of adsorbent materials.[31] Morphological analyses indicated that the surface area (3.5 $m^2\ g^{-1}$), pore size (1.7 nm) and pore volume (0.06 $cm^3\ g^{-1}$) of MHC were lower than those of HC (Table 1). Elemental analysis of MHC revealed that several important cations such as Al, Fe, Ca and Mg were found in relatively high concentrations (Table 1), suggesting that ion exchange might be an important factor in the adsorption process.

SEM images of HC and MHC (Fig. 1) indicated the presence of spherical aggregates on rough surfaces which comprised heterogeneous pores and cavities. It appeared that acid treatment of the MHC resulted in a rougher and more irregular surface than that of the HC with different shapes of wrinkles and cavities, exposing more adsorption sites for metal binding.

The FTIR spectrum of HC (Fig. 2) showed a broad O—H vibration band between 3500 and 3100 cm^{-1}, aliphatic and aromatic C—H stretching bands between 3100 and 2850 cm^{-1} with C═C aromatic stretching bands evident at 1600 and 1440 cm^{-1}.[1,32] However the intensity of these peaks significantly deceased for MHC, indicating changes in surface chemistry. In addition, several noticeable differences in the FTIR spectra between HC and MHC were observed in the fingerprint region. Peaks presented at 1063 and 1019 cm^{-1} (C═O) for HC[1,28]; however, in the case of MHC these were narrower and shifted to higher frequencies, 1156 and 1100 cm^{-1}, indicating that sulfoxide groups were formed.[24] Additionally new peaks for MHC appeared at around 1250 and 676 cm^{-1} which could be attributed to the stretching vibration of —SO_3 and mineral compounds.[8,24,33] The FTIR spectrum of Cr(VI)-loaded MHC (Fig. 2) showed broadened peaks at 1156 and 1100 cm^{-1} corresponding to sulfoxide groups, while the peaks at 1250 and 676 cm^{-1} disappeared, indicating interaction with the Cr(IV) species. Thus, structural changes after loading Cr(VI) into the composite MHC suggested that the surface functional groups play a key role in Cr(VI) adsorption.

Optimisation of adsorption conditions

Solution chemistry such as pH and ionic strength, together with process conditions such as contact time, initial adsorbate concentration, adsorbent dosage and temperature are important factors that control adsorption processes.[2] Thus, their effects on Cr(VI) removal were assessed and optimised.

Effect of solution pH

It is expected that treatment of HC with H_2SO_4 will lead to the formation of both sulfonyl groups and potentially a number of oxygen and nitrogen moieties on the HC surface.[34] Elemental composition evidence (Table 1) indicates a sulfur elemental composition of 4.4 wt% and nitrogen of 4.9 wt% on the MHC material, most likely this indicating the formation of sulfonyl groups and a variety of more basic nitrogen moieties on the MHC surface. Further evidence of the formation of sulfonyl sites is provided via the FTIR results where new peaks at around 1250 and 676 cm^{-1} were observed for MHC which could be attributed to the stretching vibration of —SO_3 and mineral compounds.[8,24,33] Also, the presence of the —SO_3H functional group was identified by the stretching vibration of S═O bond at *ca* 1156 and 1019 cm^{-1}. Nitrogen-based surface functionalities can be seen with the presence of a broad FTIR peak with midpoint at approximately 3300 cm^{-1} potentially indicating the presence of a basic amide surface functionality.[34] Following the adsorption process in the current work, in the FTIR spectrum of Cr(VI)-loaded MHC (Fig. 2) the specific peaks at 1250 and 676 cm^{-1} disappeared, indicating interaction with the Cr(VI) adsorbed species. The measured adsorption capacities (q_e) of HC and MHC at pH 2 were 9.6 and 21.7 mg g^{-1}, respectively, but decreased sharply and converged as the solution pH increased resulting in almost no adsorption at pH 6 (Fig. 3(A)). This is consistent with other batch studies which also reported maximum Cr(VI) adsorption in acidic environments[8,35,36] and can be explained by considering the surface charges of the adsorbents and the Cr(VI) adsorbate species.[2] The surface charge of an adsorbent is determined by pH_{pzc} where an adsorbent surface is neutral at $pH = pH_{pzc}$, but develops a positive charge at $pH < pH_{pzc}$ and a negative charge at $pH > pH_{pzc}$.[2] Therefore at pH 2 both HC and MHC had positive surface charges; however, as solution pH increased, the positive charges reduced and became negative[3] once the pH values increased above their

Table 1. Structural parameters and chemical composition of PL-derived HC and MHC used in this study ($n = 3$)

Parameter	HC	MHC	Ref.
Surface area ($m^2\ g^{-1}$)	7.1	3.5	17
Pore size (nm)	4.4 ± 0.6	1.7 ± 0.1	
Pore volume ($cm^3\ g^{-1}$)	0.07	0.06	
pH	7.4 ± 0.1	5.0 ± 0.3	
Ash (% w/w on dry basis)	30.2 ± 0.5	22.7 ± 0.0	
Elemental composition (% w/w on dry basis)			
C	51.4 ± 0.2	56.2 ± 0.5	22
S	0.4 ± 0.0	4.4 ± 0.0	
N	5.1 ± 0.0	4.9 ± 0.0	
Mg	0.1 ± 0.0	0.1 ± 0.0	
Ca	8.8 ± 0.0	6.3 ± 0.6	
P	4.8 ± 0.9	1.7 ± 0.1	
Fe	0.19 ± 0.0	0.20 ± 0.0	
Al	0.64 ± 0.0	0.75 ± 0.0	

Journal of Chemical Technology and Biotechnology published by John Wiley & Sons Ltd on behalf of Society of Chemical Industry (SCI).

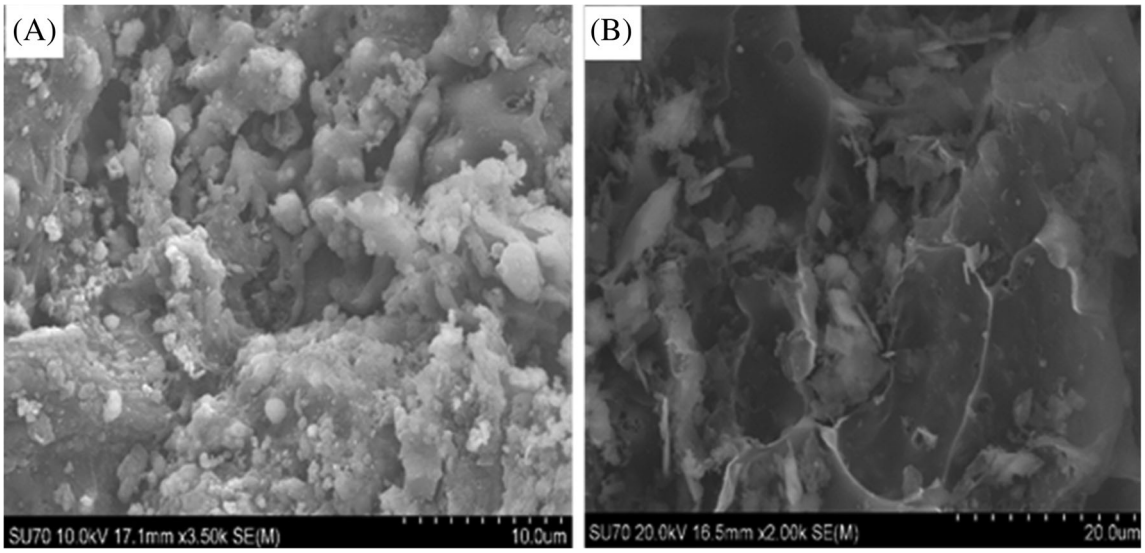

Figure 1. Morphology of HCs observed from SEM images of (A) PL-derived HC and (B) MHC.[17]

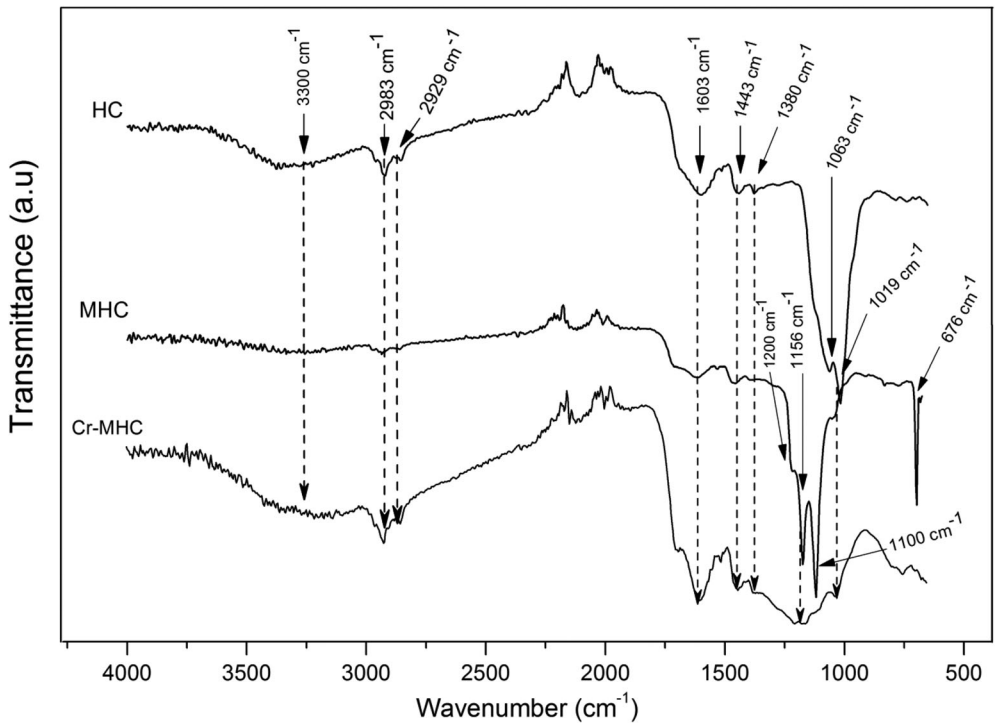

Figure 2. FTIR spectra of HC, MHC and Cr(VI)-loaded MHC (Cr-MHC).

respective pH_{pzc} (pH 7.4 and 5.9) (Fig. 3(B)). In addition, the main ionic forms of chromate at acidic pH (pH 1.0–6.8) are hydrogen chromate ($HCrO_4^-$) and dichromate ($Cr_2O_7^{2-}$) with chromate (CrO_4^{2-}) being predominant at pH > 6.8 and this results in an electrostatic attraction to the positively charged groups present on the adsorbent surface.[25,37] In contrast, increasing solution pH led to a decrease in the Cr(VI) uptake due to the deprotonation of surface functional groups, along with competition between the Cr(VI) ions and the OH^- ions to occupy the active sites.[5,38] Given the enhanced adsorption of Cr(VI) onto MHC at pH 2 (Fig. 3(A)), no further adsorption experiments were carried out on the HC, and the remainder of this study focused on Cr(VI) removal by MHC using a pH 2 solution as optimal.

Based on the evidence, it appears that the principal binding process is one of an electrostatic interaction between the sulfonyl moieties and the binding Cr(VI) species. A variety of potential mechanisms for Cr(VI) adsorption have been presented in the literature.[39-41] At low Cr(VI) adsorbate concentrations (<100 mg L^{-1}), it is expected that straight Cr(VI) adsorption would occur and that there would be a lower probability of

Journal of Chemical Technology and Biotechnology published by John Wiley & Sons Ltd on behalf of Society of Chemical Industry (SCI).

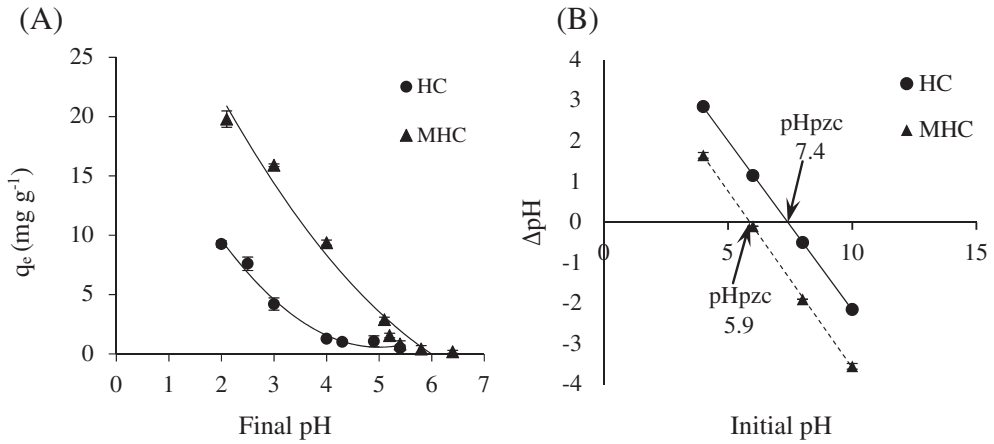

Figure 3. Effect of solution pH on (A) Cr(VI) adsorption by HC and MHC and (B) zero point charge (pH_{pzc}) of HC and MHC at 293 K. Error bars indicate ±1 SD, $n = 3$.

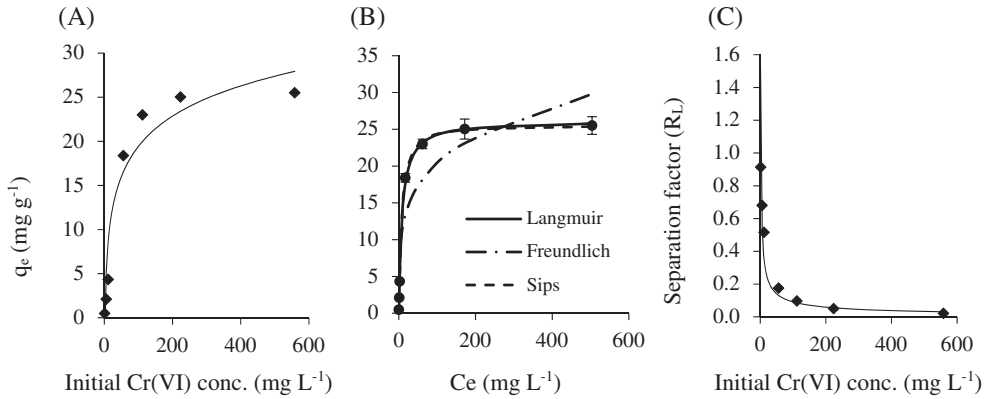

Figure 4. Plots of (A) initial Cr(VI) concentration *versus* adsorption (q_e) onto MHC, (B) Langmuir, Freundlich and Sips isotherm models fitted to adsorption data and (C) Langmuir separation factor (R_L) *versus* initial Cr(VI) concentration. All experiments ($n = 3$) were carried out at 293 K and pH 2. Error bars indicate ±1 SD, $n = 3$.

Cr(VI) reduction to Cr(III) occurring.[39] This would be expected at the lower Cr(VI) initial concentrations in the adsorption isotherms (Fig. 4(A)). At higher Cr(VI) concentrations, a second suggested adsorption mechanism may apply where the reduction of Cr(VI) to Cr(III) may occur as a result of contact between Cr(VI) and some surface functional groups that act as electron donors.[15,39] As the adsorption solution pH increases, the surface sites on the MHC are likely to become more basic and ultimately negatively charged and this could potentially stimulate a reduction of adsorbed Cr(VI) to its Cr(III) form. As part of a third suggested mechanism, a three-step surface interaction may occur starting with Cr(VI) adsorption, then Cr(VI) reduction to Cr(III) and finally desorption and re-solubilisation of the Cr(III) in solution. This mechanism is most likely to occur as the adsorption solution pH rises and is evidenced by a significant drop in Cr(VI) adsorbed.[39]

Effect of initial adsorbate concentration and adsorption isotherms

The adsorption of Cr(VI) onto MHC increased quickly as Cr(VI) adsorbate concentration increased, reaching 18.4 mg g^{-1} at 55 mg L^{-1} Cr(VI) (Fig. 4(A)). This rapid increase was likely due to the availability of multiple unoccupied active sites on the surface of MHC[3] which became saturated and unavailable at higher initial Cr(VI) concentration. In addition some of the low-energy adsorbent sites may have been mobilised by the increasing Cr(VI) ion concentration in aqueous solution. By observation, an optimum initial Cr(VI) concentration of 55 mg L^{-1} was selected for experiments relating to kinetics, thermodynamics, ionic competition and regeneration.

A plot of adsorption (q_e) *versus* equilibrium Cr(VI) concentration (C_e) represented a Type I isotherm to which the two-parameter Langmuir and Freundlich models and the three-parameter Sips model (Eqns (2)–(4) respectively) were fitted using nonlinear analysis[1,2] (Fig. 4(B)):

$$q_e = \frac{q_m K_L C_e}{1 + K_L} \tag{2}$$

$$q_e = K_F C_e^{1/n} \tag{3}$$

$$q_e = \frac{K_s C_e^{\beta_s}}{1 + \alpha_s C_e^{\beta_s}} \tag{4}$$

where q_e and q_m (mg g^{-1}) are the experimental and the maximum saturated monolayer adsorption capacities respectively, C_e (mg L^{-1}) is the equilibrium Cr(VI) concentration in solution, K_L (L mg^{-1}) is the Langmuir constant relating to the adsorption energy, K_F (L g^{-1}) and n are Freundlich constants relating to

Journal of Chemical Technology and Biotechnology published by John Wiley & Sons Ltd on behalf of Society of Chemical Industry (SCI).

adsorption capacity and adsorption energy respectively, K_s (L g^{-1}) and α_s (L mg^{-1}) are the Sips isotherm model constants and β_s is the Sips isotherm model exponent.[42-44] The Redlich–Peterson model was also fitted to the data; however, the optimum (dimensionless) g value for this model was found to be 1 and therefore reduced to the Langmuir isotherm model,[45] which together with the Sips model were found to be the best fits (Table 2; Fig. 4(B)).

The maximum adsorption capacity (26.2 mg g^{-1}) was higher than that reported using apple wood biochar (*ca* 9 mg g^{-1})[46] and using Zn- and Al-modified bamboo sawdust HCs (14 and 12.3 mg g^{-1} respectively)[47] under similar experimental conditions but lower than that for KOH-modified eucalyptus sawdust biochar (up to 45.9 mg g^{-1}).[48] The Freundlich model indicated favourable adsorption (i.e. $n > 1$) of Cr(VI) onto MHC[49] and because of the very strong correlation of the Langmuir model with the data, this was further investigated using a dimensionless separation factor (R_L)[50]:

$$R_L = \frac{1}{(1+K_L C_0)} \quad (5)$$

Table 2. Langmuir, Freundlich and Sips isotherm model constants, and statistical parameters of Cr(VI) adsorption onto MHC. All experiments were carried out at pH 2 and 293 K

Model	Parameter	Value
Langmuir	q_m (mg g^{-1})	26.21
	K_L (L mg^{-1})	0.122
	R^2	0.998
	χ^2	0.691
Freundlich	K_F (mg g^{-1})/(mg L^{-1})	6.825
	n	4.221
	R^2	0.859
	χ^2	11.662
Sips	K_s (L g^{-1})	2.484
	α_s (L mg^{-1})	0.097
	β_s	1.148
	R^2	0.999
	χ^2	1.294

where K_L is the Langmuir equilibrium constant (L mg^{-1}) and C_0 (mg L^{-1}) is the initial Cr(VI) concentration. The separation factor indicates whether the adsorption is irreversible ($R_L = 0$), linear ($R_L = 1$), favourable and reversible ($0 < R_L < 1$) or unfavourable ($R_L > 1$).[1]

The concave shape of the plot of initial Cr(VI) concentration (C_0) *versus* measured adsorption rates (Fig. 4(A)) indicates favourable and reversible adsorption[38] and this is confirmed by the rapidly decreasing values of $R_L < 1$ (0.90 to 0.02) with increasing C_0 (Fig. 4(C)).

Effect of contact time and adsorption kinetics

The adsorption of Cr(VI) onto MHC (pH = 2, 293 K) proceeded at a rate of 0.035 mg g^{-1} min^{-1} in the first 6 h until it reached an uptake of 12.7 mg g^{-1}. Between 6 and 24 h the average adsorption rate reduced to 0.007 mg g^{-1} min^{-1} to reach an uptake of 19.7 mg g^{-1}. The adsorption rate slowed considerably to just 0.001 mg g^{-1} min^{-1} between 24 and 72 h, likely due to increased saturation of all the available active sites with Cr(VI) ions, where it reached an equilibrium of 22 mg g^{-1} (Fig. 5). On this basis a contact time of 24 h, when most of adsorption took place, was used for all subsequent batch experiments.

To evaluate the kinetics of Cr(VI) adsorption onto MHC, the pseudo-first-order (PFO)[51] and pseudo-second-order (PSO)[52] models (Eqns (6) and (7) respectively) were fitted to the experimental data and the kinetic parameters were determined by non-linear regression (Fig. 5). The best fit of the models was established using the coefficient of determination (R^2) and the chi-squared (χ^2) value (Table 3):

$$q_t = q_e\left(1-e^{-k_1 t}\right) \quad (6)$$

$$q_t = \frac{k_2 q_e^2 t}{1+k_2 q_e t} \quad (7)$$

where q_t (mg g^{-1}) and q_e (mg g^{-1}) are the adsorption capacities of Cr(VI) at time t (min) and equilibrium, respectively, and k_1 (min^{-1}) and k_2 (g mg^{-1} min^{-1}) are the kinetic rate constants of the PFO and PSO models, respectively.

The PSO model had a higher R^2 and lower χ^2 than the PFO model (Table 3) and was thus a better fit to the experimental data.

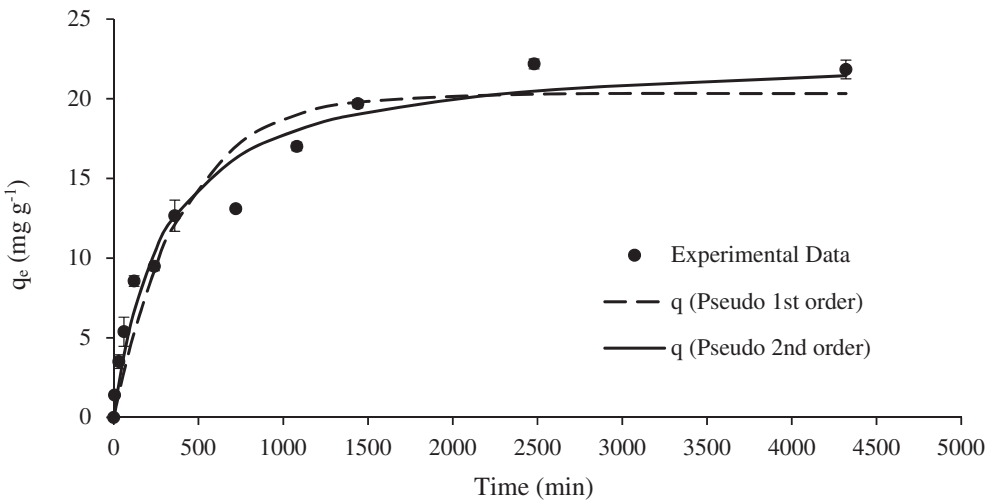

Figure 5. Adsorption kinetics of Cr(VI) onto MHC at 293 K and solution pH 2 with fitted pseudo-first-order and pseudo-second-order models. Error bars indicate ±1 SD, $n = 3$.

Journal of Chemical Technology and Biotechnology published by John Wiley & Sons Ltd on behalf of Society of Chemical Industry (SCI).

Table 3. Kinetic and statistical parameters of Cr(VI) adsorption onto MHC for pseudo-first-order and pseudo-second-order models. All experiments were carried out at pH 2 and 293 K, $n = 3$

Model	Parameter	Value
Pseudo-first-order kinetics	q_e (mg g^{-1})	20.32
	k_1 (min^{-1})	−0.0025
	R^2	0.946
	χ^2	13.630
Pseudo-second-order kinetics	q_e (mg g^{-1})	22.91
	k_2 (g mg^{-1} min^{-1})	0.0001
	R^2	0.969
	χ^2	5.641
Intraparticle diffusion	k_{i1} (mg g^{-1} min$^{-1/2}$)	0.654
	α_{i1} (mg g^{-1})	0.197
	R_1^2	0.973
	k_{i2} (mg g^{-1} min$^{-1/2}$)	0.224
	α_{i2} (mg g^{-1})	9.066
	R_2^2	0.809
Boyd	R^2 ($0 \le t \le 6$ h)	0.960

This suggests that multiple removal mechanisms such as ion exchange, electrostatic attraction and surface complexation may be involved in the removal process, consistent with previous findings.[46]

However while the PSO model describes the kinetic data, it does not provide sufficient insight into the adsorption mechanisms. The four main adsorption mechanisms are (i) bulk transport – this occurs instantaneously and is generally considered negligible as a rate-limiting process; (ii) film diffusion – this is the transfer of solutes through a hydrodynamic boundary layer via a concentration gradient onto the surface of the adsorbent; (iii) intraparticle diffusion – once on the boundary of the adsorbent, the solutes diffuse along and into the pores of the adsorbent, provided they are sufficiently large; and (iv) adsorptive attachment – this is attachment of the molecules to the pores which occurs very quickly and is also considered negligible as a rate-limiting process.[45] Therefore in order to elucidate between film and intraparticle diffusion, a linearised form of the intraparticle diffusion model[53] (Eqn (8)) was used:

$$q_t = k_i t^{1/2} + \alpha \tag{8}$$

where k_i (mg g^{-1} min$^{-1/2}$) is the intraparticle diffusion rate constant and α (mg g^{-1}) is the equilibrium constant associated with the boundary layer thickness.[45,53] If a straight line intercepts the origin in a plot of q_t *versus* $t^{1/2}$, then only intraparticle diffusion controls the adsorption process; however, if multiple linear regions are indicated then adsorption is controlled by multistage mechanisms. In this study two linear regions were identified (Fig. 6(A)) indicating that at least two steps influenced the adsorption process. The first linear region ($t \le 360$ min), representing film diffusion, occurs at a higher rate than the second region which represents intraparticle diffusion ($k_{i1} > k_{i2}$) (Table 3). This may be due to the initially high concentration gradient which reduces with time as MHC becomes saturated with Cr(VI) ions. In addition the equilibrium constant for the second region is higher than that for the first region ($\alpha_{i2} > \alpha_{i1}$) (Table 3), indicating that boundary layer effects become more limiting as time increases.[54,55]

To establish whether film diffusion or intraparticle diffusion is the rate-limiting step for adsorption of Cr(VI) onto MHC, the Boyd model[56] was used (Eqns (9) and (10)). This model assumes that the adsorption process is governed by intraparticle diffusion if a plot of Bt against time is linear and passes through the origin; otherwise film diffusion governs the sorption process:

$$Bt = -\ln\frac{\pi^2}{6} - \ln(1 - F(t)), \text{for } F(t) > 0.85 \tag{9}$$

$$Bt = \left(\sqrt{\pi} - \sqrt{\pi - \frac{\pi^2 F(t)}{3}}\right)^2, \text{for } F(t) \le 0.85 \tag{10}$$

where Bt is Boyd's number and $F(t) = q/q_e$ at time t.

A plot of the Boyd model (Fig. 6(B)) shows that at $t \le 6$ h, the plot is linear and passes through the origin, indicating that

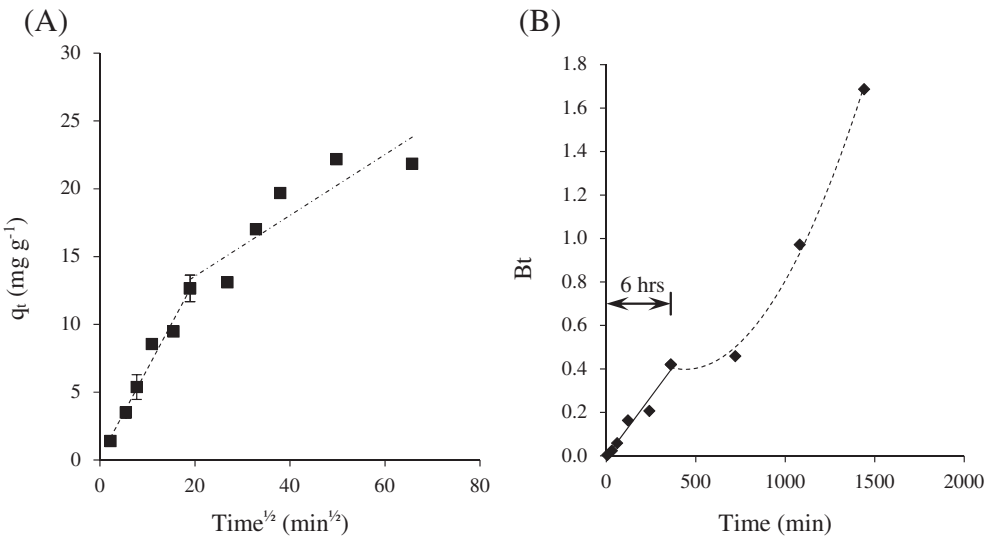

Figure 6. (A) Intraparticle diffusion model and (B) Boyd model for adsorption of Cr(VI) onto MHC at 293 K and solution pH 2. Error bars indicate ±1 SD, $n = 3$.

Journal of Chemical Technology and Biotechnology published by John Wiley & Sons Ltd on behalf of Society of Chemical Industry (SCI).

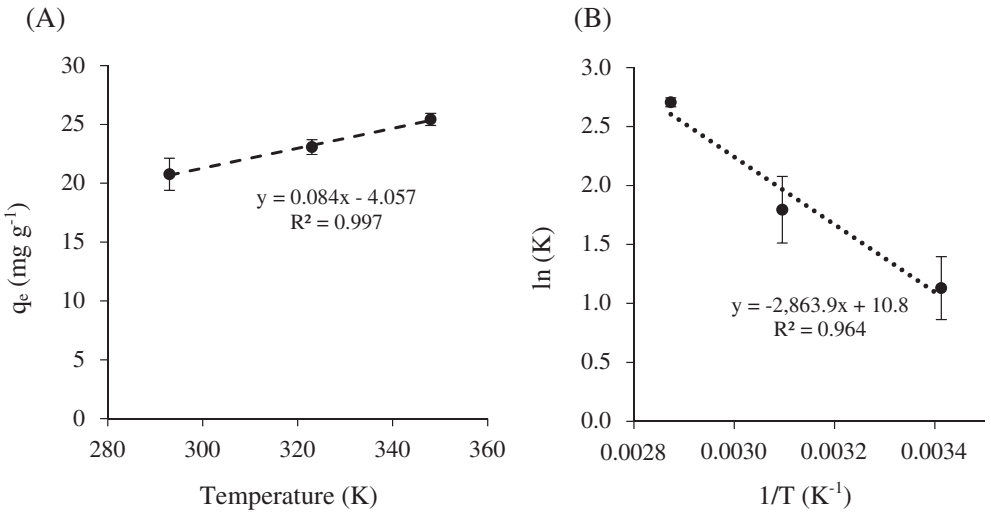

Figure 7. (A) Uptake of Cr(VI) *versus* temperature onto MHC using 30 mL of 55 mg L^{-1} Cr(VI) solution at pH 2 and MHC application rate of 2 g L^{-1}. (B) Arrhenius plot for adsorption of Cr(VI) onto MHC in the range 293–348 K. Error bars indicate ±1 SD, $n = 3$.

Table 4. Thermodynamic parameters of adsorption of Cr(VI) onto MHC

	Thermodynamic parameters			
Temperature (K)	K_c	$\Delta G°$ (kJ mol^{-1})	$\Delta H°$ (kJ mol^{-1})	$\Delta S°$ (J mol^{-1} K^{-1})
293	3.17	−2.75	23.81	90.07
323	6.18	−4.82		
348	14.96	−7.83		

intraparticle diffusion is rate limiting for this period. Thereafter film diffusion governs the process as the model becomes non-linear at $t \geq 6$ h. The rate-limiting process can also be viewed from the perspective of solute concentration. The equilibrium Cr(VI) concentration at $t = 5$ min was 53 ± 0.16 mg L^{-1} and this reduced to 29 ± 1.81 mg L^{-1} after 360 min. It can be postulated therefore that above a critical equilibrium concentration of 30 mg L^{-1} Cr(VI), intraparticle diffusion is rate limiting, reflective of the high concentration gradient, while below this equilibrium concentration film diffusion becomes rate limiting, reflective of the reduced concentration gradient.[55,56]

Effect of temperature and adsorption thermodynamics

The biosorption of Cr(VI) onto MHC increased moderately and linearly from 20.76 to 25.42 mg g^{-1} as the solution temperature increased from 293 to 348 K, indicating an endothermic process (Fig. 7(A)). The higher temperature may have increased the mobility of Cr(VI) ions, facilitating their adsorption onto active sites of MHC[7] while elevated temperatures may also help to generate and expose more functional groups, increasing the ability of MCH to adsorb Cr(VI).[57]

To further examine the effects of temperature on the adsorption of Cr(VI) onto MHC, changes to the thermodynamic parameters of Gibbs free energy $\Delta G°$ (kJ mol^{-1}), enthalpy $\Delta H°$ (kJ mol^{-1}) and entropy $\Delta S°$ (J mol^{-1} K^{-1}) were established (Eqns (11)–(14)):

$$K_c = \frac{C_0 - C_e}{C_e} \quad (11)$$

$$\Delta G° = -RT \ln K_c \quad (12)$$

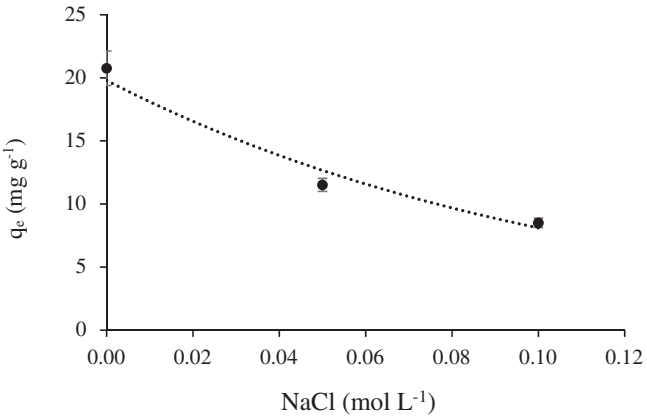

Figure 8. Effect of NaCl addition on adsorption of Cr(VI) solution onto MHC. All experiments were carried out using 30 mL of 55 mg L^{-1} Cr(VI) at pH 2 mixed with varying concentrations of NaCl (0.00, 0.05 and 0.1 mol L^{-1}), at 293 K and stirred with 2 g L^{-1} MHC for 24 h. Error bars indicate ±1 SD, $n = 3$.

$$\Delta G° = \Delta H° - T\Delta S° \quad (13)$$

$$\ln K = \frac{\Delta S°}{R} - \frac{\Delta H°}{RT} \quad (14)$$

where K_c is the thermodynamic equilibrium constant, C_0 and C_e are the initial and equilibrium Cr(VI) concentrations (mg L^{-1}) respectively, T (K) is the temperature of the adsorption process and R (8.314 J mol^{-1} K^{-1}) is the universal gas constant. The values

Journal of Chemical Technology and Biotechnology published by John Wiley & Sons Ltd on behalf of Society of Chemical Industry (SCI).

Table 5. Adsorption–desorption cycles of Cr(VI) onto MHC. All experiments ($n = 3$) were carried out at 293 K with adsorption at pH 2 and desorption at pH 12

	Cr(VI) concentration (mg L^{-1})		
Cycle no.	Initial	Final	Cr(VI) adsorption (mg g^{-1})
Initial	55.83 ± 0.82	10.03 ± 0.07	22.26 ± 0.40
Regeneration 1	55.27 ± 1.12	3.07 ± 0.02	23.83 ± 0.19
Regeneration 2	56.12 ± 1.38	4.69 ± 0.63	24.41 ± 0.30
Regeneration 3	55.29 ± 1.27	14.39 ± 0.18	20.59 ± 0.14
Regeneration 4	55.83 ± 1.16	16.55 ± 0.22	19.21 ± 0.69

of ΔH° and ΔS° were obtained from the slope and intercept, respectively, of a plot of ln K *versus* $1/T$ (van't Hoff equation)[1,2] (Fig. 7(B); Table 4).

The ΔG° values for the adsorption of Cr(VI) onto MHC were negative and decreased with temperature, indicating that the adsorption process was spontaneous (i.e. occurs without an external energy input) and the removal efficiency was favoured at high temperature.[2] The positive values of ΔH° confirmed the endothermic nature of the adsorption[22] while the low enthalpy change ($\Delta H^\circ < 40$ kJ mol^{-1}) suggested that the adsorption of Cr(VI) onto MHC was a physisorption process.[2] The entropy change was positive ($\Delta S^\circ = 90.07$ J mol^{-1} K^{-1}) indicating that adsorption of Cr(VI) onto MHC became more random during the adsorption process.[22]

Effect of ionic strength

Adsorption is influenced by electrostatic interactions between the adsorbent surface and adsorbate ions and this may be affected by competing species, such as NaCl, which typically exist in significant quantities in contaminated water.[7] Increasing NaCl concentrations in the Cr(VI) adsorbate from 0.0 to 0.1 mol L^{-1} led to a nonlinear decrease in the adsorption capacity of Cr(VI) from 20.8 to 8.5 mg g^{-1} (Fig. 8). This is probably due to competition between Na^+ ions and positively charged adsorbent sites for the negatively charged Cr(VI) ions.[58] In addition the Na^+ could hinder the electrostatic attraction between the charges on the adsorbent and Cr(VI) ions in solution and confirms the role of electrostatic attraction in the adsorption of Cr(VI) onto MHC. A similar observation was reported in a study of the effect of background electrolyte cations (Na^+, K^+, Ca^{2+} and Mg^{2+}) on the adsorption of Cr(VI) onto β-cyclodextrin/poly(L-glutamic acid)-modified ramie biochar. This was attributed to the presence of cations hindering the electrostatic interaction between active sites on the biochar surface and Cr(VI) ions and the competition between Cr(VI) and Cl^- for adsorption sites.[59]

Regeneration and reuse

While adsorption of Cr(VI) using MHC is environmentally beneficial, desorption is an additional step not only for Cr(VI) recovery but also to assess the reusability of MHC. The adsorption–desorption cycle was repeated four times with results indicating consistent removal rates over all cycles (Table 5). The ability of Cr(VI) to desorb from MHC further supports the finding that it is loosely bound on the surface, indicating that MHC demonstrates reasonable regeneration and reusable potential for the adsorption of Cr(VI).

CONCLUSIONS

MHC was effective at removing Cr(VI) from aqueous solution. The maximum adsorption capacity (26.2 mg g^{-1}) was achieved at a solution pH of 2 and was well fitted with the Langmuir isotherm model. The kinetic data followed the PSO model indicating that electrostatic interactions, ion exchange and redox processes might be involved in the removal process. The Cr(VI) ions were first adsorbed onto the MHC surface by electrostatic attraction between Cr(VI) ions mainly in the form $HCrO_4^-$ and protonated functional groups at low pH. At the same time, adsorbed Cr(VI) reduced partly to Cr(III) cations by the electron-donor groups which increased its positive charge, leading to further increase in the electronic attraction between Cr(VI) ions and functional groups. This explained the optimal acid condition (pH 2) for Cr(VI) adsorption. The relatively rapid initial uptake coupled with its potential for regeneration indicated that this biosorbent is a promising low-cost, environmentally friendly means of removing Cr(VI) from contaminated waters while simultaneously providing an alternative outlet for highly polluting PL. However, further studies, such as a lifecycle assessment, would be required to determine its overall environmental, ecological and economic impacts prior to large-scale production.

ACKNOWLEDGEMENT

BG acknowledges the financial support provided by the Libyan government as a postgraduate research grant.

REFERENCES

1 Ghanim B, O'Dwyer TF, Leahy JJ, Willquist K, Courtney R, Pembroke JT *et al.*, Application of KOH modified seaweed hydrochar as a biosorbent of vanadium from aqueous solution: characterisations, mechanisms and regeneration capacity. *J Environ Chem Eng* **8**:104176 (2020). https://doi.org/10.1016/j.jece.2020.104176.
2 Ghanim B, Murnane JG, O'Donoghue L, Courtney R, Pembroke JT and O'Dwyer TF, Removal of vanadium from aqueous solution using a red mud modified saw dust biochar. *J Water Process Eng* **33**:101076 (2020). https://doi.org/10.1016/j.jwpe.2019.101076.
3 Tangtubtim S and Saikrasun S, Adsorption behavior of polyethyleneimine-carbamate linked pineapple leaf fiber for Cr(VI) removal. *Appl Surf Sci* **467**:596–607 (2019). https://doi.org/10.1016/j.apsusc.2018.10.204.
4 Jawed A, Saxena V and Pandey LM, Engineered nanomaterials and their surface functionalization for the removal of heavy metals: a review. *J Water Process Eng* **33**:101009 (2020). https://doi.org/10.1016/j.jwpe.2019.101009.
5 Xia S, Song Z, Jeyakumar P, Shaheen SM, Rinklebe J, Ok YS *et al.*, A critical review on bioremediation technologies for Cr(VI)-contaminated soils and wastewater. *Crit Rev Environ Sci Technol* **49**:1027–1078 (2019). https://doi.org/10.1080/10643389.2018.1564526.

6 Pakade VE, Tavengwa T and Madikizela LM, Recent advances in hexavalent chromium removal from aqueous solutions by adsorptive methods. *RSC Adv* **9**:26142–26164 (2019). https://doi.org/10.1039/c9ra05188k.

7 Xia S, Song Z, Wang H, Jeyakumar P and Bolan N, Characteristics and applications of biochar for remediating Cr(VI)-contaminated soils and wastewater. *Environ Geochem Health* **42**:1543–1567 (2020). https://doi.org/10.1007/s10653-019-00445-w.

8 Wei J, Tu C, Yuan G, Bi D, Xiao L, Theng BKG *et al.*, Carbon-coated montmorillonite nanocomposite for the removal of chromium(VI) from aqueous solutions. *J Hazard Mater* **368**:541–549 (2019). https://doi.org/10.1016/j.jhazmat.2019.01.080.

9 Li HY, Yang Y, Zhang M, Wei W and Xie B, A novel anion exchange method based on in situ selectively reductive desorption of Cr(VI) for its separation from V(V): toward the comprehensive use of hazardous wastewater. *J Hazard Mater* **368**:670–679 (2019). https://doi.org/10.1016/j.jhazmat.2019.01.099.

10 European Innovation Partnership on Raw Materials. *Raw Materials Scoreboard 2018*. European Union (2018). Available: https://biblio.ugent.be/publication/8529540/file/8529541 [August 2021].

11 Kim E, Spooren J, Broos K, Nielsen P, Horckmans L, Geurts R *et al.*, Valorization of stainless steel slag by selective chromium recovery and subsequent carbonation of the matrix material. *J Clean Prod* **117**:221–228 (2016). https://doi.org/10.1016/j.jclepro.2016.01.032.

12 Spooren J, Binnemans K, Björkmalm J, Breemersch K, Dams Y, Folens K *et al.*, Near-zero-waste processing of low-grade, complex primary ores and secondary raw materials in Europe: technology development trends. *Resour Conserv Recycl* **160**:104919 (2020). https://doi.org/10.1016/j.resconrec.2020.104919.

13 Lyu H, Tang J, Huang Y, Gai L, Zeng EY, Liber K *et al.*, Removal of hexavalent chromium from aqueous solutions by a novel biochar supported nanoscale iron sulfide composite. *Chem Eng J* **322**:516–524 (2017). https://doi.org/10.1016/j.cej.2017.04.058.

14 Masoumi S, Borugadda VB, Nanda S and Dalai AK, Hydrochar: a review on its production technologies and applications. *Catalysts* **11**:939 (2021). https://doi.org/10.3390/catal11080939.

15 Hu B, Ai Y, Jin J, Hayat T, Alsaedi A, Zhuang L *et al.*, Efficient elimination of organic and inorganic pollutants by biochar and biochar-based materials. *Biochar* **2**:47–64 (2020). https://doi.org/10.1007/s42773-020-00044-4.

16 Barquilha CE and Braga MC, Adsorption of organic and inorganic pollutants onto biochars: challenges, operating conditions, and mechanisms. *Bioresour Technol Rep* **15**:100728 (2021). https://doi.org/10.1016/j.biteb.2021.100728.

17 Ghanim BM, Pandey DS, Kwapinski W and Leahy JJ, Hydrothermal carbonisation of poultry litter: effects of treatment temperature and residence time on yields and chemical properties of hydrochars. *Bioresour Technol* **216**:373–380 (2016). https://doi.org/10.1016/j.biortech.2016.05.087.

18 Shao Y, Tan H, Shen D, Zhou Y, Jin Z, Zhou D *et al.*, Synthesis of improved hydrochar by microwave hydrothermal carbonization of green waste. *Fuel* **266**:117146 (2020). https://doi.org/10.1016/j.fuel.2020.117146.

19 Mau V and Gross A, Energy conversion and gas emissions from production and combustion of poultry-litter-derived hydrochar and biochar. *Appl Energy* **213**:510–519 (2018). https://doi.org/10.1016/j.apenergy.2017.11.033.

20 Reza MT, Andert J, Wirth B, Busch D, Pielert J, Lynam JG *et al.*, Hydrothermal carbonization of biomass for energy and crop production. *Appl Bioenergy* **1**:11–29 (2014). https://doi.org/10.2478/apbi-2014-0001.

21 Fang J, Zhan L, Ok YS and Gao B, Minireview of potential applications of hydrochar derived from hydrothermal carbonization of biomass. *J Ind Eng Chem* **57**:15–21 (2018). https://doi.org/10.1016/j.jiec.2017.08.026.

22 Shi Y, Zhang T, Ren H, Kruse A and Cui R, Polyethylene imine modified hydrochar adsorption for chromium(VI) and nickel(II) removal from aqueous solution. *Bioresour Technol* **247**:370–379 (2018). https://doi.org/10.1016/j.biortech.2017.09.107.

23 Han L, Sun H, Ro KS, Sun K, Libra JA and Xing B, Removal of antimony(III) and cadmium(II) from aqueous solution using animal manure-derived hydrochars and pyrochars. *Bioresour Technol* **234**:77–85 (2017). https://doi.org/10.1016/j.biortech.2017.02.130.

24 Ghanim BM, Kwapinski W and Leahy JJ, Hydrothermal carbonisation of poultry litter: effects of initial pH on yields and chemical properties of hydrochars. *Bioresour Technol* **238**:78–85 (2017). https://doi.org/10.1016/j.biortech.2017.04.025.

25 Kabir MM, Mouna SSP, Akter S, Khandaker S, Didar-ul-Alam M, Bahadur NM *et al.*, Tea waste based natural adsorbent for toxic pollutant removal from waste samples. *J Mol Liq* **322**:115012 (2021). https://doi.org/10.1016/j.molliq.2020.115012.

26 Severini F, Leahy JJ and Kwapinski W, Heterogeneous char based solid acid catalysts from brown bin waste to create a green process for the production of butyl butyrate. *Waste Biomass Valorization* **8**:2431–2441 (2017). https://doi.org/10.1007/s12649-016-9696-9.

27 Vithanage M, Rajapaksha AU, Zhang M, Thiele-Bruhn S, Lee SS and Ok YS, Acid-activated biochar increased sulfamethazine retention in soils. *Environ Sci Pollut Res* **22**:2175–2186 (2015). https://doi.org/10.1007/s11356-014-3434-2.

28 Qian L and Chen B, Interactions of aluminum with biochars and oxidized biochars: implications for the biochar aging process. *J Agric Food Chem* **62**:373–380 (2014). https://doi.org/10.1021/jf404624h.

29 Ghanim BM, Kwapinski W and Leahy JJ, Speciation of nutrients in hydrochar produced from hydrothermal carbonization of poultry litter under different treatment conditions. *ACS Sustain Chem Eng* **6**:11265–11272 (2018). https://doi.org/10.1021/acssuschemeng.7b04768.

30 Qi F, Yan Y, Lamb D, Naidu R, Bolan NS, Liu Y *et al.*, Thermal stability of biochar and its effects on cadmium sorption capacity. *Bioresour Technol* **246**:48–56 (2017). https://doi.org/10.1016/j.biortech.2017.07.033.

31 Heidari M, Dutta A, Acharya B and Mahmud S, A review of the current knowledge and challenges of hydrothermal carbonization for biomass conversion. *J Energy Inst* **92**:1779–1799 (2019). https://doi.org/10.1016/j.joei.2018.12.003.

32 Lang Q, Guo Y, Zheng Q, Liu Z and Gai C, Co-hydrothermal carbonization of lignocellulosic biomass and swine manure: hydrochar properties and heavy metal transformation behavior. *Bioresour Technol* **266**:242–248 (2018). https://doi.org/10.1016/j.biortech.2018.06.084.

33 Yacou C, Altenor S, Carene B and Gaspard S, Chemical structure investigation of tropical *Turbinaria turbinata* seaweeds and its derived carbon sorbents applied for the removal of hexavalent chromium in water. *Algal Res* **34**:25–36 (2018). https://doi.org/10.1016/j.algal.2018.06.014.

34 Islam MT, Hyder AG, Saenz-Arana R, Hernandez C, Guinto T, Ahsan MA *et al.*, Removal of methylene blue and tetracycline from water using peanut shell derived adsorbent prepared by sulfuric acid reflux. *J Environ Chem Eng* **7**:102816 (2019). https://doi.org/10.1016/j.jece.2018.102816.

35 Zhao J, Boada R, Cibin G and Palet C, Enhancement of selective adsorption of Cr species via modification of pine biomass. *Sci Total Environ* **756**:143816 (2021). https://doi.org/10.1016/j.scitotenv.2020.143816.

36 Chang J, Wang H, Zhang J, Xue Q and Chen H, New insight into adsorption and reduction of hexavalent chromium by magnetite: multistep reaction mechanism and kinetic model developing. *Colloids Surf A* **611**:125784 (2021). https://doi.org/10.1016/j.colsurfa.2020.125784.

37 Zhou L, Liu Y, Liu S, Yin Y, Zeng G, Tan X *et al.*, Investigation of the adsorption-reduction mechanisms of hexavalent chromium by ramie biochars of different pyrolytic temperatures. *Bioresour Technol* **218**:351–359 (2016). https://doi.org/10.1016/j.biortech.2016.06.102.

38 Dragan ES, Humelnicu D, Dinu MV and Olariu RI, Kinetics, equilibrium modeling, and thermodynamics on removal of Cr(VI) ions from aqueous solution using novel composites with strong base anion exchanger microspheres embedded into chitosan/poly(vinyl amine) cryogels. *Chem Eng J* **330**:675–691 (2017). https://doi.org/10.1016/j.cej.2017.08.004.

39 Valentín-Reyes J, García-Reyes RB, García-González A, Soto-Regalado E and Cerino-Córdova F, Adsorption mechanisms of hexavalent chromium from aqueous solutions on modified activated carbons. *J Environ Manage* **236**:815–822 (2019). https://doi.org/10.1016/j.jenvman.2019.02.014.

40 Wang H, Guo H, Zhang N, Chen Z, Hu B and Wang X, Enhanced photoreduction of U(VI) on C_3N_4 by Cr(VI) and bisphenol A: ESR, XPS, and EXAFS investigation. *Environ Sci Technol* **53**:6454–6461 (2019). https://doi.org/10.1021/acs.est.8b06913.

41 Zhu Y, He X, Xu J, Fu Z, Wu S, Ni J *et al.*, Insight into efficient removal of Cr(VI) by magnetite immobilized with *Lysinibacillus* sp. JLT12: mechanism and performance. *Chemosphere* **262**:127901 (2021). https://doi.org/10.1016/j.chemosphere.2020.127901.

Journal of Chemical Technology and Biotechnology published by John Wiley & Sons Ltd on behalf of Society of Chemical Industry (SCI).

42 Wang W, Chromium(VI) removal from aqueous solutions through powdered activated carbon countercurrent two-stage adsorption. *Chemosphere* **190**:97–102 (2018). https://doi.org/10.1016/j.chemosphere.2017.09.141.

43 Sips R, Combined form of Langmuir and Freundlich equations. *J Chem Phys* **16**:490–495 (1948).

44 Foo KY and Hameed BH, Insights into the modeling of adsorption isotherm systems. *Chem Eng J* **156**:2–10 (2010). https://doi.org/10.1016/j.cej.2009.09.013.

45 Tran HN, You SJ, Hosseini-Bandegharaei A and Chao HP, Mistakes and inconsistencies regarding adsorption of contaminants from aqueous solutions: a critical review. *Water Res* **120**:88–116 (2017). https://doi.org/10.1016/j.watres.2017.04.014.

46 Liu N, Zhang Y, Xu C, Liu P, Lv J, Liu YY *et al.*, Removal mechanisms of aqueous Cr(VI) using apple wood biochar: a spectroscopic study. *J Hazard Mater* **384**:121371 (2020). https://doi.org/10.1016/j.jhazmat.2019.121371.

47 Li F, Zimmerman AR, Hu X and Gao B, Removal of aqueous Cr(VI) by Zn- and Al-modified hydrochar. *Chemosphere* **260**:127610 (2020). https://doi.org/10.1016/j.chemosphere.2020.127610.

48 Zhang X, Zhang L and Li A, Eucalyptus sawdust derived biochar generated by combining the hydrothermal carbonization and low concentration KOH modification for hexavalent chromium removal. *J Environ Manage* **206**:989–998 (2018). https://doi.org/10.1016/j.jenvman.2017.11.079.

49 Anandaraj B, Eswaramoorthi S, Rajesh TP, Aravind J and Babu PS, Chromium(VI) adsorption by *Codium tomentosum*: evidence for adsorption by porous media from sigmoidal dose–response curve. *Int J Environ Sci Technol* **15**:2595–2606 (2018). https://doi.org/10.1007/s13762-017-1488-7.

50 Hall KR, Eagleton LC, Acrivos A and Vermeulen T, Pore- and solid-diffusion kinetics in fixed-bed adsorption under constant-pattern conditions. *Ind Eng Chem Fundam* **5**:212–223 (1966). https://doi.org/10.1021/i160018a011.

51 Lagergren S, Zur theorie der sogenannten adsorption gelˆster stoffe, Kungliga Svenska Vetenskapsakademiens. *Handlingar* **24**:1–39 (1898).

52 Blanchard G, Maunaye M and Martin G, Removal of heavy metals from waters by means of natural zeolites. *Water Res* **18**:1501–1507 (1984). https://doi.org/10.1016/0043-1354(84)90124-6.

53 Weber WJ and Morris JC, Kinetics of adsorption on carbon from solution. *J Sanit Eng Div* **89**:31–60 (1963). https://doi.org/10.1061/JSEDAI.0000430.

54 McKay G and Otterburn MS, The removal of colour from effluent using various adsorbents – III. Silica: rate processes. *Water Res* **14**:15–20 (1980). https://doi.org/10.1016/0043-1354(80)90037-8.

55 Hubbe MA, Azizian S and Douven S, Implications of apparent pseudo-second-order adsorption kinetics onto cellulosic materials: a review. *BioResources* **14**:7582–7626 (2019). https://doi.org/10.15376/biores.14.3.7582-7626.

56 Boyd GE, Adamson AW and Myers LS Jr, The exchange adsorption of ions from aqueous solutions by organic zeolites. II. Kinetics. *J Am Chem Soc* **69**:2836–2848 (1947). https://doi.org/10.1021/ja01203a066.

57 Kar S and Equeenuddin SM, Adsorption of hexavalent chromium using natural goethite: isotherm, thermodynamic and kinetic study. *J Geol Soc India* **93**:285–292 (2019). https://doi.org/10.1007/s12594-019-1175-z.

58 Rosales E, Meijide J, Pazos M and Sanromán MA, Challenges and recent advances in biochar as low-cost biosorbent: from batch assays to continuous-flow systems. *Bioresour Technol* **246**:176–192 (2017). https://doi.org/10.1016/j.biortech.2017.06.084.

59 Jiang L, Liu S, Liu Y, Zeng G, Guo Y, Yin Y *et al.*, Enhanced adsorption of hexavalent chromium by a biochar derived from ramie biomass (*Boehmeria nivea* (L.) Gaud.) modified with *β*-cyclodextrin/poly(L-glutamic acid). *Environ Sci Pollut Res* **24**:23528–23537 (2017). https://doi.org/10.1007/s11356-017-9833-4.

